

## Significant improvement of activation energy in MgB<sub>2</sub>/Mg<sub>2</sub>Si multilayer films

Y. Zhao<sup>a)</sup> and S. X. Dou

*Institute for Superconducting and Electronic Materials, University of Wollongong, Wollongong, NSW 2522, Australia*

M. Ionescu

*Australian Nuclear Science and Technology Organization (ANSTO), Menai, NSW 2234, Australia*

P. Munroe

*Electron Microscope Unit, University of New South Wales, Sydney, NSW 2052, Australia*

(Received 3 May 2005; accepted 8 November 2005; published online 3 January 2006)

We obtained a MgB<sub>2</sub>/Mg<sub>2</sub>Si multilayer structure by sequentially switching a stoichiometric MgB<sub>2</sub> target and a Si target during off-axis pulsed-laser deposition. The transmission-electron-microscopic cross-sectional image of the resulting film exhibits a layered structure with each MgB<sub>2</sub> layer being 40–50 nm thick and the Mg<sub>2</sub>Si interlayers about 5 nm thick. A clearly enhanced anisotropy in the irreversibility lines and the vortex activation energy was observed. Pinning and the flux flow activation energy are significantly increased in parallel applied fields. © 2006 American Institute of Physics. [DOI: 10.1063/1.2159572]

With a layered structure, a superconductor usually shows different behaviors from that of bulk, such as the crossover from three-dimensional to two-dimensional upper critical field ( $H_{c2}$ ) behavior,<sup>1–3</sup> the scaling effect in the angular dependence of critical current density ( $J_c$ ),<sup>4</sup> and enhanced anisotropy in the vortex pinning energy.<sup>5</sup> These phenomena can be a good tool in revealing the pinning mechanism and superconducting parameters for superconductors. Lawrence and Doniach<sup>6</sup> have proposed a weak Josephson coupling model for superconductor/insulator superlattices. The model was then extensively studied by Klemm *et al.*<sup>1</sup> and extended into superconductor/normal conductor superlattices by Takahashi and Tachiki.<sup>2</sup> The model explains successfully the temperature dependence of the upper critical field of the superconducting superlattices and intrinsically layered high-temperature superconductors (HTSs). There have been a number of experimental reports on multilayered low temperature superconductors<sup>3,7–9</sup> and HTS.<sup>10–13</sup> The newly discovered moderate temperature superconductor MgB<sub>2</sub> has a layered structure and two separate superconducting gaps.<sup>14,15</sup> The Ginzburg–Landau (GL) coherence length  $\xi(0)$  is about 10 nm within  $a$ - $b$  plane and 5 nm along  $c$  axis for MgB<sub>2</sub>.<sup>16</sup> Because that the coupling between B layers in MgB<sub>2</sub> ( $c=0.352$  nm) are strong, the superconductor is not expected to display intrinsic two-dimensional pancake vortices that have been predicted in HTS.<sup>17</sup> In this letter, we show that using sequential pulsed laser deposition (PLD), an artificially multilayered structure has been achieved with the aid of an off-axis deposition method.<sup>18</sup> The MgB<sub>2</sub>/Mg<sub>2</sub>Si multilayer structure leads to a significant enhancement of pinning and the activation energy  $U_0$  when the applied field is parallel to the  $a$ - $b$  plane of the film.

In the PLD process, a stoichiometric MgB<sub>2</sub> target (84% density), a Si target and a magnesium target were set on a carousel in the chamber. The laser beam was generated by an excimer laser system (Lambda-Physik) operating on KrF gas

( $\lambda=248$  nm, 25 ns). The chamber was first evacuated to a base vacuum of about  $8 \times 10^{-8}$  Torr and then filled with high-purity argon to 120 mTorr as the background gas. Before the deposition, the heater was kept at 250 °C. Sapphire  $c$ -cut substrates with dimensions of about  $6 \times 2$  mm<sup>2</sup> were used. With an off-axis geometry,<sup>18</sup> the substrate is parallel to the normal axis of the target surface and aligned to the center of the laser spot. The substrate is mounted onto the edge of the heater with silver paste. We switched the MgB<sub>2</sub> and Si targets ten times during the deposition. At the end of the deposition, the Mg target was switched to the depositing position to provide a protective Mg cap layer. Then the Ar pressure was increased to 760 Torr before the *in situ* annealing. The films were heated to 650 °C in 12 min and kept at that temperature for 1 min. For comparison, monolayer MgB<sub>2</sub> films are prepared under the same conditions and referred as MgB<sub>2</sub> film in the following text. The resulting films have a thickness of 400–500 nm, as detected by atomic force microscope (AFM) and transmission electron microscope (TEM).

The conductive measurements were carried out using a four-probe method with a dc current density of 10 A/cm<sup>2</sup>. In both the  $H \parallel ab$ -plane (parallel field) and  $H \perp ab$ -plane (perpendicular field) cases, the testing current was perpendicular to the applied field.

Figure 1 shows a bright-field (BF) TEM image of the cross-sectional view of the Si-added film. The film exhibits a layered structure, where each MgB<sub>2</sub> layer is 40–50 nm thick and the interlayers are about 5 nm thick. Each MgB<sub>2</sub> layer consists of very fine grains. Individual grains are less than 20 nm in size. A similar equiaxial fine-grain structure was also observed in our MgB<sub>2</sub> films. The inset of Fig. 1 is a selected area electron diffraction (SAED) image of the film with the incident beam at a particular angle from the  $c$ -axis of the film. The divided MgB<sub>2</sub> rings indicate a textured grain structure with MgB<sub>2</sub> (0001) parallel to the film plane, the same orientation of our MgB<sub>2</sub> films.<sup>18</sup> The 5 nm thick interlayers between the 10 MgB<sub>2</sub> layers are Mg<sub>2</sub>Si, judging from the electron diffraction and x-ray energy dispersive spectroscopy.

<sup>a)</sup>Electronic mail: yz70@uow.edu.au

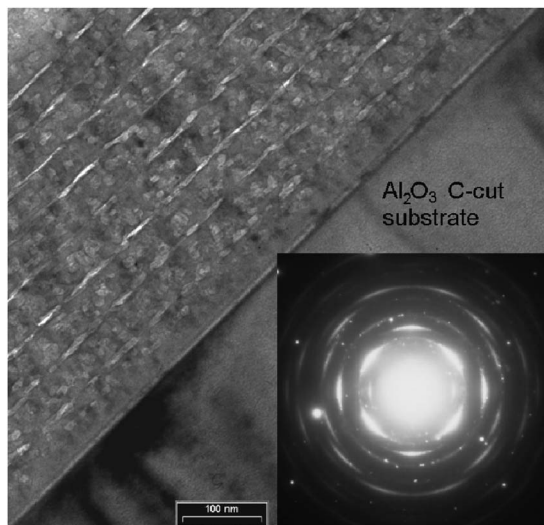


FIG. 1. BF TEM image of the multilayer film. The scale bar is 100 nm. The inset is an SAED of the  $\text{MgB}_2$  film, showing a clear textured grain orientation.

copy (EDS) results. The existence of  $\text{Mg}_2\text{Si}$  is in accordance with the previous reports on Si addition in the Mg-B system.<sup>19,20</sup>

EDS detection of the whole cross-sectional area of the multilayer film shows an average atomic ratio Si:Mg of 1:19. By assuming only  $\text{MgB}_2$  and  $\text{Mg}_2\text{Si}$  phases are present in the multilayered film, the Si addition level is estimated to be 3.5 wt. % and the volume ratio  $\text{Mg}_2\text{Si}:\text{MgB}_2$  about 1:8.3. This result is in accordance with the thickness ratio of  $\text{Mg}_2\text{Si}/\text{MgB}_2$  observed in Fig. 1, indicating that the added Si in  $\text{MgB}_2$  films remain predominantly in the  $\text{Mg}_2\text{Si}$  interlayers.

The  $T_c$  of the multilayer film is slightly suppressed by  $\sim 1.5$  K compared with the  $\text{MgB}_2$  film, as shown in Fig. 2. The zero resistivity  $T_c$  of the multilayer film is 31 K. The transition widths from 10%  $\rho(40$  K) to 90%  $\rho(40$  K) for both films are the same, about 0.5 K. The narrow transition width of the multilayered film indicates that the  $\text{MgB}_2$  phase remains homogenous after the addition of Si. The values of the resistivity of the multilayer film are generally 1.5 times the residual resistivity of the undoped film in the temperature

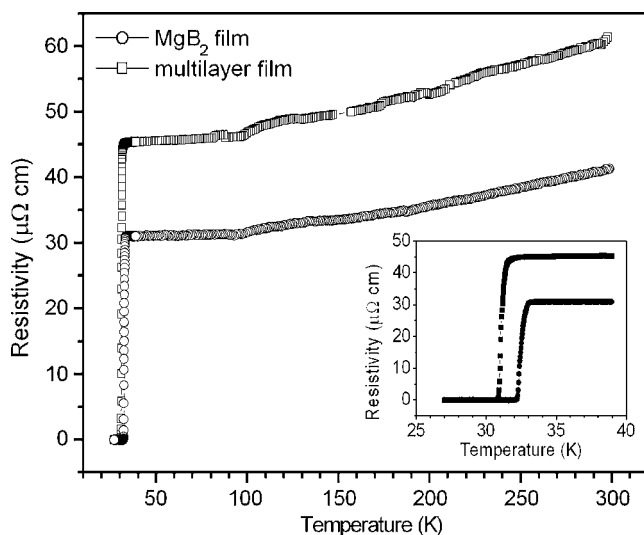


FIG. 2. Resistivity vs temperature curves of multilayer film and  $\text{MgB}_2$  film.

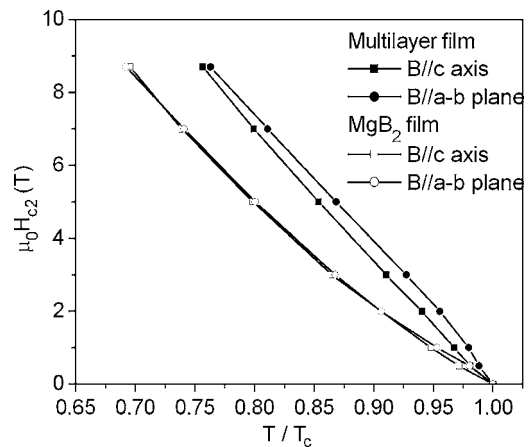


FIG. 3. The  $H_{c2}$  vs  $T/T_c$  for the multilayered film and  $\text{MgB}_2$  film.

range of 32 K–300 K. As pointed out by Rowell *et al.*,<sup>21</sup> the rise of the resistivity may indicate a reduction of the effective current carrying area or an increased defect level in the Si added film.

Figure 3 shows the upper critical fields of the multilayer film and the  $\text{MgB}_2$  film. The fact that the  $H_{c2}$  anisotropy of our  $c$ -oriented  $\text{MgB}_2$  film is highly suppressed might be a result of the strong intragrain scattering that is usually observed in the *in situ* PLD  $\text{MgB}_2$  films. The upper critical fields in different temperatures are derived from the 90%  $\rho_{T_c}$  points in the  $\rho$ - $T$  curves. The  $H_{C2}^{ab}$  and  $H_{C2}^c$  of the multilayer film are clearly increased, which may indicate that more intragrain scattering is introduced by Si addition. As predicted by Takahashi *et al.*,<sup>2</sup> the  $H_{C2}^{ab}$  of a layered superconductor will be much higher than the  $H_{C2}^c$  when the thickness of superconducting layers and normal layers is comparable to the coherence length  $\xi(0)$  of the superconductor. A single  $\text{MgB}_2$  layer is 40–50 nm thick for our multilayer film, much larger than the  $\xi(0)$  of the  $\text{MgB}_2$  layer. Therefore, the multilayer film did not show a pronounced two-dimensional behavior of  $H_{c2}$ .

The irreversibility fields of the multilayer film and the  $\text{MgB}_2$  film are derived from transport curves using the 10%  $\rho_{T_c}$  values and shown in Fig. 4. The irreversibility field  $H_{irr}^c$  for the multilayer film is almost identical to the  $H_{irr}^{ab}$  and  $H_{irr}^c$  of the  $\text{MgB}_2$  film, showing the same level of flux pinning in the three circumstances. However, the  $H_{irr}^{ab}$  of the multilayer

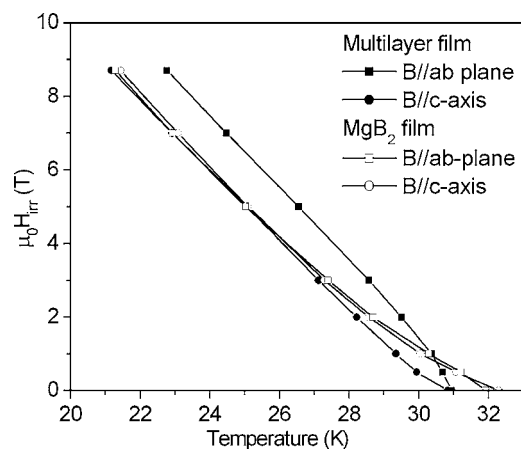


FIG. 4. The irreversibility fields of the multilayer film and the  $\text{MgB}_2$  film.

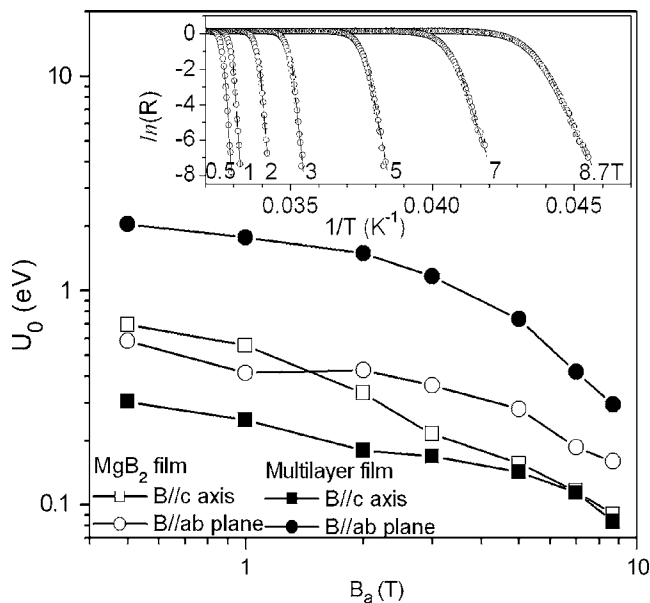


FIG. 5. The activation energy,  $U_0$  of flux flow versus applied field,  $B_a$ . The inset shows the Arrhenius plot of resistance  $R(T, H)$  for the multilayer film in parallel fields.

film is clearly increased, indicating a significant enhancement of pinning in parallel fields.

Although the activation energy of the thermally assisted flux flow (TAFF) for  $\text{MgB}_2$  is significantly higher than that of HTS, TAFF is still detectable through the resistivity-temperature curves for different applied fields. The activation energy  $U_0$  of our  $\text{MgB}_2$  and multilayer films is estimated by Arrhenius law,<sup>22–24</sup>  $\rho = \rho_0 \exp(-U_0/k_B T)$ , where  $\rho_0$  is a field-independent pre-exponential factor, and  $k_B$  is the Boltzmann's constant. The Arrhenius fits of resistance  $R(T, H)$  for the multilayer film in parallel fields are shown in the inset of Fig. 5. The straight part of the  $\ln(R)-1/T$  curves represents the TAFF regime. Figure 5 shows the activation energy of flux flow versus applied field,  $B_a$ . An enhanced anisotropy of  $U_0$  is clearly revealed. The activation energy of the  $\text{MgB}_2$  film is 0.6–0.7 eV in the low-field regime for both perpendicular and parallel fields.  $U_0$  is significantly increased in the multilayer film (about 2 eV in the low-field regime) when the applied field is parallel to the  $a$ - $b$  plane of the film. The thickness of the nonsuperconducting  $\text{Mg}_2\text{Si}$  interlayer is typically 5 nm, of the same order as  $\xi_{ab}(0)$  of  $\text{MgB}_2$ . The coupling of vortices across the  $\text{Mg}_2\text{Si}$  layer is relatively weak. When the applied field is parallel to the  $a$ - $b$  plane, the vortices are probably trapped in the nonsuperconducting  $\text{Mg}_2\text{Si}$  layers. Thus, the two-dimensional  $\text{Mg}_2\text{Si}$  defect both provides strong flux pinning and increases the thermal activation energy for flux flow in the parallel field. The activation energy for the multilayer film is decreased in perpendicular fields compared with the  $\text{MgB}_2$  film, which may imply an easier TAFF due to the vortex decoupling across

the non-superconductive interlayers that has been observed and studied in HTS and other artificially multilayered superconducting films.<sup>5,10</sup>

In conclusion, the 5 nm thick  $\text{Mg}_2\text{Si}$  interlayers provide effective flux pinning for the  $\text{MgB}_2/\text{Mg}_2\text{Si}$  multilayer film in parallel fields. An enhanced anisotropy of the flux activation energy  $U_0$  is observed in the multilayer film.  $U_0$  is significantly increased when the applied field is perpendicular to the  $c$  axis and the testing current, which is in accordance with the enhancement of  $H_{irr}^{ab}$ ,  $H_{c2}$  and the residual resistance are clearly increased, which may indicate that some defects and intra-band scattering is introduced by Si addition.

The authors thank J. Horvat, A. V. Pan, and T. Silver for their help in this work. The work was supported by the Australian Research Council, Hyper Tech Research Inc, OH, Alphatech International Ltd, NZ, and the University of Wollongong.

- <sup>1</sup>R. A. Klemm, A. Luther, and M. R. Beasley, *Phys. Rev. B* **12**, 877 (1975).
- <sup>2</sup>S. Takahashi and M. Tachiki, *Phys. Rev. B* **33**, 4620 (1986).
- <sup>3</sup>M. G. Karkut, V. Matijasevic, L. Antognazza, J. M. Triscone, N. Missert, M. R. Beasley, and O. Fischer, *Phys. Rev. Lett.* **60**, 1751 (1988).
- <sup>4</sup>G. Jakob, M. Schmitt, T. Kluge, C. Tomerosa, P. Wagner, T. Hahn, and H. Adrian, *Phys. Rev. B* **47**, 12099 (1993).
- <sup>5</sup>J. R. Clem, *Supercond. Sci. Technol.* **11**, 909 (1998).
- <sup>6</sup>W. E. Lawrence and S. Doniach, in *Proceedings of the 12th International Conference on Low Temperature Physics*, Tokyo, 1971 (Academic, Japan, 1971), p. 361.
- <sup>7</sup>S. T. Ruggiero, T. W. Barbee, Jr., and M. R. Beasley, *Phys. Rev. Lett.* **45**, 1299 (1980).
- <sup>8</sup>J. M. Murduck, D. W. C. II, I. K. Schuller, S. Foner, and J. B. Ketterson, *Appl. Phys. Lett.* **52**, 504 (1988).
- <sup>9</sup>I. K. Schuller, *Phys. Rev. Lett.* **44**, 1597 (1980).
- <sup>10</sup>J. L. Martin, M. Velez, and J. L. Vicent, *Phys. Rev. B* **52**, R3872 (1995).
- <sup>11</sup>K.-H. Kim, H.-J. Kim, S.-I. Lee, A. Iyo, Y. Tanaka, K. Tokiwa, and T. Watanabe, *Phys. Rev. B* **70**, 92501 (2004).
- <sup>12</sup>P. N. Barnes, T. J. Haugan, C. V. Varanasi, and T. A. Campbell, *Appl. Phys. Lett.* **85**, 4088 (2004).
- <sup>13</sup>J. Hanisch, C. Cai, R. Huhne, L. Schultz, and B. Holzapfel, *Appl. Phys. Lett.* **86**, 122508 (2005).
- <sup>14</sup>I. I. Mazin and V. P. Antropov, *Physica C* **385**, 49 (2003).
- <sup>15</sup>H. J. Choi, M. L. Cohen, and S. G. Louie, *Physica C* **385**, 66 (2003).
- <sup>16</sup>A. D. Caplin, Y. Bugoslavsky, L. F. Cohen, L. Cowey, J. Driscoll, J. Moore, and G. K. Perkins, *Supercond. Sci. Technol.* **16**, 176 (2003).
- <sup>17</sup>J. R. Clem, *Supercond. Sci. Technol.* **5**, S33 (1992).
- <sup>18</sup>Y. Zhao, M. Ionescu, J. Horvat, and S. X. Dou, *Supercond. Sci. Technol.* **18**, 395 (2005).
- <sup>19</sup>X. L. Wang, S. H. Zhou, M. J. Qin, P. R. Munroe, S. Soltanian, H. K. Liu, and S. X. Dou, *Physica C* **385**, 461 (2003).
- <sup>20</sup>L. D. Cooley, K. Kang, R. Klie, Q. Li, A. Moodenbaugh, and R. Sabatini, *Supercond. Sci. Technol.* **17**, 942 (2004).
- <sup>21</sup>J. M. Rowell, S. Y. Xu, X. H. Zeng, A. V. Pogrebnikov, Q. Li, X. X. Xi, J. M. Redwing, W. Tian, and X. Pan, *Appl. Phys. Lett.* **83**, 102 (2003).
- <sup>22</sup>T. M. Palstra, B. Batlogg, R. B. v. Dover, L. F. Schneemeyer, and J. V. Waszczak, *Appl. Phys. Lett.* **54**, 763 (1989).
- <sup>23</sup>T. M. Palstra, B. Batlogg, R. B. v. Dover, L. F. Schneemeyer, and J. V. Waszczak, *Phys. Rev. B* **41**, 6621 (1990).
- <sup>24</sup>A. Sidorenko, V. Zdravkov, V. Ryazanov, S. Horn, S. Klimm, R. Tidecks, A. Wixforth, T. Koch, and T. Schimmel, *cond-mat/0406062* (2004).